Preventing heat injuries by predicting individualized human core temperature

Srinivas Laxminarayan,[1] Vineet Rakesh,[1] Mark J. Buller,[2] William J. Tharion,[2] Jaques Reifman[1]

[1]Department of Defense Biotechnology High Performance Computing Software Applications Institute, Telemedicine and Advanced Technology Research Center, U.S. Army Medical Research and Materiel Command, Fort Detrick, MD 21702, USA

[2]U.S. Army Research Institute of Environmental Medicine, Biophysics and Biomedical Modeling Division, Natick, MA 01760, USA

slaxminarayan@bhsai.org; vineetrakesh@gmail.com; mark.j.buller.civ@mail.mil; william.j.tharion.civ@mail.mil; jaques.reifman.civ@mail.mil

ABSTRACT

Heat injury is a problem for the Armed Forces, especially during deployment to localities with very hot and humid climates. Early warning of a rising core body temperature (T_C) can help prevent heat injuries. To this end, we developed an algorithm that, given a series of past T_C measurements obtained using an ingestible temperature pill, accumulates evidence of a rising T_C over time and provides ahead-of-time warning of an impending, dangerously elevated T_C. Using data from a cohort of six Soldiers involved in field exercises whose T_C exceeded 38.5°C, we assessed the performance of the warning algorithm. The algorithm predicted rises in T_C with a clinically useful lead time (> 18 min) and reasonable sensitivity and specificity (> 87%). However, because ingestible temperature pills are impractical for monitoring a large number of Warfighters during prolonged operations, we developed a mathematical model that uses non-invasive measurements of physiological variables, such as activity (A_C), heart rate (H_R), and skin temperature, as well as environmental information [ambient temperature (T_A) and relative humidity (R_H)], to provide individualized real-time T_C estimates. Using the same cohort of Soldiers, we evaluated two variants of the individualized model, one that used all the measurements (original model) and another that used A_C, H_R, and month-average T_A and R_H values (reduced model). The original and reduced models yielded T_C estimates with average errors of 0.31°C and 0.35°C, respectively, which are within the physiological intra-subject variability of T_C. In addition, on average, the estimation time delays ranged from 3 min for the original model to 5 min for the reduced model. We conclude that the individualized T_C estimation model can be used to replace ingestible temperature pills and enable the development of a field-deployable early warning system of an impending rise in core temperature.

1.0 INTRODUCTION

Heat-related illnesses are a significant problem for the United States (U.S.) Armed Forces, especially during deployments to localities with hot and humid climates. In fact, between 2009 and 2013 there were 12,907 heat injuries across the Services, including 1,757 cases of heat stroke [1, 2]. The primary sign of an impending heat injury is a rise in core body temperature (T_C). However, during strenuous military operations in hot and humid conditions, Warfighters focused on their mission could miss warning signs of an increasing T_C and an impending heat illness [3]. New sensor technologies, which afford the ability to measure T_C via ingestible temperature pills [4], and mathematical predictive models [5, 6] could be coupled to develop a hardware/software warning system of an impending rise in T_C and generate alerts to potentially prevent heat injuries.

Although ingestible temperature pills provide accurate T_C measurements, they are invasive and cannot be used for continuously monitoring large number of Warfighters during prolonged operations. This has led to the investigation of more practical alternatives, such as the use of non-invasive performance- and fitness-tracking devices that monitor a wide range of physiological variables, e.g., activity (A_C), heart rate (H_R), and skin temperature (T_S), which can then be used to indirectly infer T_C. This could be accomplished by a physiology-based mathematical model that combines the information from such non-invasive measurements using phenomenological and first-principles concepts to provide individualized T_C estimates in real time.

In this study, we report on the development of algorithms to address the two requirements for developing a reliable early warning system for heat injury prevention: *1*) an algorithm that, given a time series of T_C measurements or T_C estimates, provides ahead-of-time alerts about an impending rise in T_C and *2*) an individualized model that uses non-invasive measurements of A_C, H_R, and T_S as well as two environmental variables [ambient temperature (T_A) and relative humidity (R_H)] to provide real-time T_C estimates.

2.0 T_C PREDICTION AND ALERT ALGORITHMS

Here, we detail the development of an algorithm that uses a time series of recent-past T_C measurements to provide reliable, ahead-of-time alerts of an impending rise in T_C.

2.1 Methods: T_C Prediction and Alert Algorithms

2.1.1 Study Data

To demonstrate the performance of the proposed algorithm, we used data from a field study involving six U.S. Army Soldiers [average age: 23.1 year (standard deviation [SD] 4.1); average height: 178 cm (SD 7); average weight: 81.3 kg (SD 11.1)] who performed regularly scheduled infantry training. The training included a six-mile foot march while wearing a backpack and carrying equipment weighing on average 14.0 kg (SD 1.4) and exercises, such as digging ditches, setting-up concertina wire, performing marksmanship drills, running, rolling, and jumping as part of the approach to a target. During the training, which lasted for 8 to 14 h, Soldiers wore the advanced combat uniform with a thermal insulation of 1.08 clo and an evaporative potential of 0.41 im/clo. During the training period, the recorded average T_A was 29.3°C (SD 2.1), the average R_H was 74% (SD 11), and the average wind speed was 2.5 m/s (SD 0.8). All training was at the direction of the military unit, i.e., the research team did not interfere with or ask for any alteration to training events. The Institutional Review Board of the U.S. Army Research Institute of Environmental Medicine (Natick, MA) approved the study.

Each Soldier was instrumented with radio-thermometer pills (MiniMitter, Inc., Bend, OR) that measured and transmitted core temperature data to the Hidalgo Equivital EQ-02 (Hidalgo, Ltd., Cambridge, UK) physiological status monitoring (PSM) system [7]. Data were retrieved from the PSM system at the end of the exercise and subsequently analyzed. Soldiers ingested the pills at least 12 h before data collection. The thermometer pills had the following technical characteristics: length: 21.9 mm; diameter: 8.5 mm; weight: 1.75 grams; sampling period: 15 s; temperature range 32°C – 42°C, with an accuracy of ±0.1°C; transmission method: near-field magnetic link. Additionally, the PSM system measured the following three physiological variables: *1*) A_C via triaxial accelerometers, *2*) H_R via two electrocardiogram electrodes, and *3*) T_S via an infrared sensor.

2.1.2 Auto-regressive (AR) Model

Given temperature measurements $T_{C_{t-i}}$ at discrete time t sampled every S min, where $i = 0, 1,\ldots, m\text{-}1$, the AR model of order m predicts T_C at time point t+1, $\hat{T}_{C_{t+1}}$, through a linear combination of the antecedent T_C

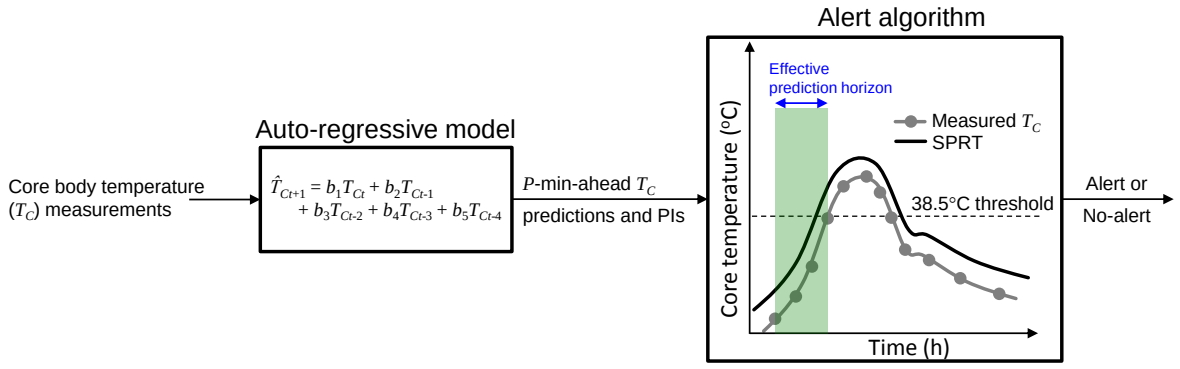

Figure 1: The sequential probability ratio test (SPRT) algorithm that provides alerts of an impending rise in core body temperature (T_C). The auto-regressive (AR) model uses a history of recent T_C measurements to make a *P*-min-ahead predictions. It also provides the corresponding prediction intervals (PIs), i.e., the uncertainty of the predictions. The SPRT algorithm uses the AR model outputs to decide whether T_C would rise beyond a predefined temperature threshold and provides ahead-of-time alerts if it does.

samples and AR model coefficients b (see Figure 1). To make predictions M time-steps ahead (prediction window $P = M \times S$ min ahead), we iteratively used the AR model equation M times, substituting the unobserved signals at $t \geq t+1$ by their corresponding predicted values. In this study, we set the sampling period $S = 5$ min to preserve the important frequencies while rejecting high-frequency noise in the magnitude spectrum of the T_C data. Subsequently, we set the AR model order $m = 5$, the number of lags in the data beyond which the partial autocorrelation function was essentially zero.

We used the measured T_C data from a subject to estimate b using the standard forward-backward least squares method (see [8], chapter 8) implemented in MATLAB version 7.14 (function *ar*). We also estimated the prediction intervals (PIs) that provide information about the uncertainty of the predicted values. To estimate the PIs, we used a statistical bootstrap method, where a population of models is built based on blocks of data that are randomly drawn from the original time series to form an empirical distribution of models (i.e., a distribution of the model coefficients) [9]. Following this procedure, we estimated the covariance matrix Σ of the AR model from a distribution of models for an M time-step-ahead predictor, and used the following equation to estimate the PIs [10]:

$$\mathrm{PI} = Z_{\alpha/2}\sqrt{y^T \Sigma y + \sigma^2}\,, \tag{1}$$

where $Z_{\alpha/2}$ denotes the prediction factor associated with an α% type I error, y represents a vector of data samples $y = [T_{C_t}\ T_{C_{t-1}}\ \ldots\ T_{C_{t-m+1}}]^T$, and σ^2 denotes the variance of the measurement noise. For detailed information about the AR model and computation of the PIs, please refer to Ref. 6.

2.1.3 Sequential Probability Ratio Test Algorithm

The sequential probability ratio test (SPRT) [11] is a Bayesian approach that considers increasing evidence from a sequence of observations to decide whether T_C will rise beyond a given temperature threshold and, if so, provides an alert [12]. Briefly, given a sequence of core temperature samples $X_1, X_2, \ldots$ not necessarily independent, so that $X \sim \mathcal{N}(\mu_X, \sigma_X^2)$ is a normal Gaussian process with unknown mean μ_X and a given variance σ_X^2, the SPRT tests the null hypothesis (H_0) that $\mu_X = \mu_0$ against an alternative hypothesis (H_1) that $\mu_X = \mu_1$, where μ_0 and μ_1 denote the mean temperature values below and above the temperature threshold, respectively, with $\mu_0 < \mu_1$. If p_0 and p_1 are the probability density functions governing H_0 and H_1, respectively, then the observed likelihood ratio at decision time t can be represented as $l_t = \prod_{k=0}^{K-1} \frac{p_1(X_{t-k})}{p_0(X_{t-k})}$, where K is the length of the sequence of samples being considered.

In order to apply the SPRT algorithm to our problem, we combined three predicted values, namely, the AR-model prediction ($\hat{T}_{Ct-k}$), the upper PI ($\hat{T}_{Ct-k} + \mathrm{PI}_{t-k}$), and the lower PI ($\hat{T}_{Ct-k} - \mathrm{PI}_{t-k}$), using weights θ and ϕ to form:

$$X_{t-k} = \hat{T}_{Ct-k} - \mathrm{PI}_{t-k}(1 - \theta\phi - \phi), \quad (2)$$

where $k = (0, 1, \ldots, K-1)$ denotes a time index and the weights θ and ϕ are constrained to be between 0 and 1. In Eq. (2), when $\phi = 0$, X_{t-k} equals the lower PI; when $\phi = 1$ and $\theta = 0$, X_{t-k} equals the AR-model prediction; and when $\theta = \phi = 1$, X_{t-k} equals the upper PI. Thus, X_t lies between the lower and upper PIs for all values of θ and ϕ. Note that a decision at time t, for a prediction window of P min, is actually made at time t-P. Then, following Wald's SPRT methodology [11], we:

accepted H_0 (below temperature threshold), if $\log(l_t) < \log(B)$; or

accepted H_1 (above temperature threshold), if $\log(l_t) < \log(A)$; or

made no decision and proceeded to time t+1, if $\log(B) \leq \log(l_t) \leq \log(A)$,

where A and B are constants that control the false-positive rate and false-negative rate, respectively, with $0 < B < A < \infty$. The SPRT algorithm required the estimation of seven parameters, the two weights θ and ϕ in Eq. (2) and the five parameters μ_0, μ_1, σ_X, A, and B from a subject's core temperature data. For detailed information about the development of the SPRT algorithm, please refer to Ref. 6.

2.1.4 Evaluating the Performance of the Alert Algorithm

To evaluate the alert algorithm, we defined an "event" as an episode where the T_C measurement rises and remains above a specified temperature threshold for ≥ 15 min. The event ends when the measured temperature decreases below the threshold and remains below the threshold for ≥ 15 min. Thus, an event was mapped into a 1 (true response) when the measured temperature was above the threshold and 0 otherwise. Similarly, a model-predicted event was defined as an episode where the alert algorithm's output (the model-predicted response) was 1.

We evaluated the algorithm's performance using four measures:

(1) Sensitivity: the fraction of time points during which both the true and model-predicted responses were 1. The fraction of time points was based on the entire time series of T_C measurements.

(2) Specificity: the fraction of time points during which both the true and model-predicted responses were 0. The fraction of time points was based on the entire time series of T_C measurements.

(3) Effective prediction horizon: for each true event, we computed the effective prediction horizon by adding the prediction window P to the time difference Δt between the onset of the true event and the onset of the model-predicted event. The reported effective prediction horizon was averaged over the number of events.

(4) Number of decision switches: the cumulative number of times the model-predicted output transitioned from one state to another (0 to 1 or 1 to 0) that was incongruent with the true state (0 or 1) of the measured temperature.

We computed specificity and the number of decision switches regardless of whether or not an event had occurred, however, we only computed sensitivity and effective prediction horizon when a true event occurred. Note that while specificity measured the time period for which the algorithm incorrectly predicted the occurrence of an event, the number of decision switches provided the number of times the algorithm predictions incorrectly switched from one state to another.

We evaluated the performance of the alert algorithm on the six subjects whose T_C exceeded 38.5°C using a cross-validation approach. For this purpose, we estimated the AR model coefficients b and the SPRT parameters on one subject's T_C data, applied the algorithm on the other five subjects, and computed the four measures of performance for each of the subjects. We repeated this procedure for each of the six subjects.

2.2 Results: T_C Prediction and Alert Algorithms

Figure 2 shows a comparison of the performance of the SPRT-based alert algorithm to a 38.5°C threshold applied to one subject (subject #1). In Figure 2, the top panel shows the measured data (black dash-dot line), the 20-min-ahead AR model predictions (red dashed line), and the corresponding PIs (shaded region). The middle panel depicts the true events (black solid line) and the events predicted by Prediction+PI (red dashed line), while the bottom panel shows the same plots for the events predicted by the SPRT-based alert algorithm. Note that in this example, the parameters of the AR model and the SPRT algorithm were estimated using the T_C data from subject #6. For this example, Prediction+PI yielded 100% sensitivity, 95% specificity, four decision switches due to noisy predictions, and an effective prediction horizon of 33 min (the predicted event anticipated the true event by 13 min beyond the 20-min prediction window). SPRT yielded a 98% sensitivity, a 96% specificity, no decision switches, and an effective prediction horizon of 28 min. Thus, SPRT yielded a slightly lower sensitivity and a reduced effective prediction horizon but, importantly, produced no decision switches compared with Prediction+PI.

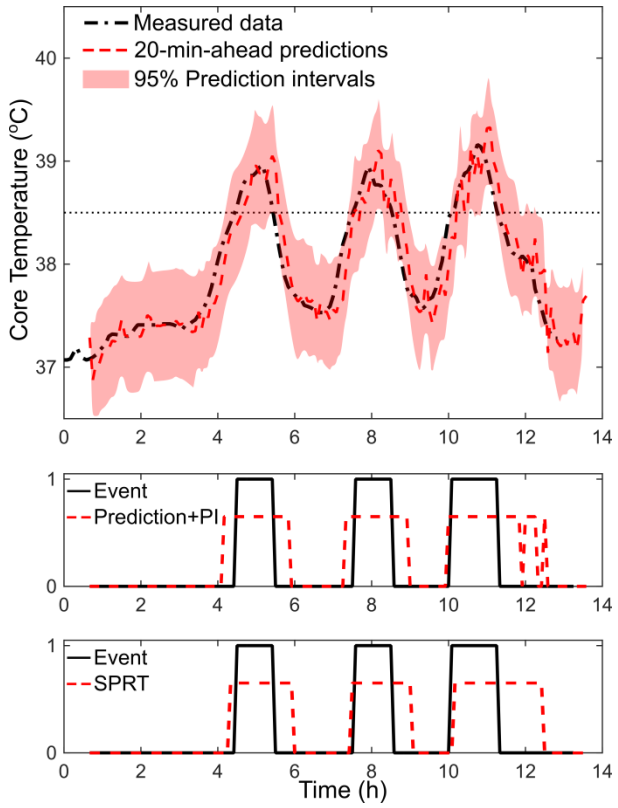

Figure 2: The top panel shows the measured core temperature data from one subject, 20-min-ahead AR model predictions, and the corresponding PIs. The middle and bottom panels show the depiction of a true event (solid black line) and algorithm decisions (dashed red line) for Prediction+PI and sequential probability ratio test (SPRT) algorithms, respectively, for a temperature threshold of 38.5°C.

Table 1: Performance of the sequential probability ratio test (SPRT) algorithm applied to 20-min-ahead auto-regressive model core body temperature predictions at a temperature threshold of 38.5°C

Algorithm	Sensitivity (%)	Specificity (%)	Effective prediction horizon (min)	Number of decision switches
Prediction+PI	100.0 (0.0)	70.6 (4.2)	33 (3)	14
SPRT	87.5 (7.6)	92.2 (8.3)	18 (7)	4

Values are means (standard deviations) from a fivefold cross-validation study of six subjects whose core body temperatures exceeded 38.5°C in 11 distinct events.

Table 1 shows a comparison of the average performance of the SPRT-based alert algorithm against the Prediction+PI algorithm across the six subjects using the cross-validation approach described in Section 2.1.4. The results suggest that SPRT increased the specificity and reduced the number of decision switches at the cost of a reduced sensitivity and effective prediction horizon.

2.3 Discussion: T_C Prediction and Alert Algorithms

While Prediction+PI yielded the largest sensitivity and the longest effective prediction horizon, it also yielded the largest number of decision switches. In contrast, delaying alert decisions through accumulation of evidence (SPRT) yielded a small number of decision switches at the cost of reduced sensitivity and effective prediction horizon. For practical applications, the 18-min effective prediction horizon yielded by SPRT provides sufficient time to enable preventive interventions to avoid the risk of heat injuries. Importantly, the SPRT algorithm yielded an increased specificity and a significant reduction in the number of decision switches and, hence, is the algorithm recommended for the development of a real-time early warning system.

3.0 INDIVIDUALIZED REAL-TIME T_C ESTIMATION USING NON-INVASIVE MEASUREMENTS

As mentioned above, a practical limitation in developing an early warning system is the use of an invasive sensor to measure T_C. To obviate the necessity of an ingestible pill, we developed a mathematical model that uses non-invasive measurements of other physiological variables and two environmental variables to provide individualized real-time T_C estimates. We detail the model below.

3.1 Methods: T_C Estimation Using Non-Invasive Measurements

3.1.1 Individualized T_C Estimation Model

The proposed individualized model uses non-invasive measurements of a subject's A_C, H_R, and T_S as well as two environmental variables, T_A and R_H, to estimate the subject's T_C in real time (Figure 3). The individualized model includes two elements: *1*) a mathematical model and *2*) a Kalman filter [13]. First, the mathematical model uses the measured A_C and environmental variables T_A and R_H to estimate the state variables H_R, T_S, and T_C. Then, the Kalman filter considers the error between the measured and model-estimated H_R and T_S to correct the state variables and update the model parameters, resulting in an improved estimation and individualization of T_C. We used data from the six subjects described in Section 2.1.1 for model development and performance evaluation.

3.1.2 The Mathematical Model

The mathematical model consists of two sub-models, a phenomenological component that relates A_C to H_R and a first-principles, macroscopic energy balance component [14] that relates the metabolic activity

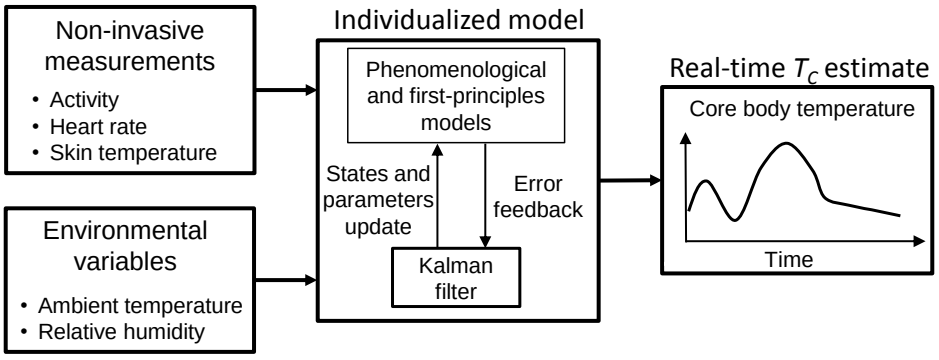

Figure 3: The individualized model for core body temperature (T_C). The inputs to the model are the measured heart rate, skin temperature, and activity profiles from a subject and two environmental variables (ambient temperature and relative humidity). The activity profile and environmental factors drive the phenomenological and first-principles models. The Kalman filter algorithm then considers the error between the measured and model-estimated heart rate and skin temperature to update the model parameters and provide individualized real-time T_C estimates.

(represented by H_R) to T_S and T_C. We computed A_C from triaxial accelerometer data provided through the PSM system by combining the three orthogonal axes (X, Y, and Z) data to obtain physical activity intensity. Then, we transformed the intensity to MET values, which is the ratio of oxygen consumed during physical activity to that at rest. Next, following the work by Sasaki et al., we quantized the MET values into five activity levels: 0 for rest (MET = 1), 1 for light activity (MET ~ 1–3), 2 for moderate activity (MET ~ 3–6), 3 for hard activity (MET ~ 6–9), and 4 for very hard activity (MET ≥ 9) [15]. Accordingly, A_C was indexed to represent values between 0 and 4. The phenomenological component was represented by a linear first-order ordinary differential equation (ODE) driven by A_C that estimated H_R.

The first-principles component consists of two ODEs. The first ODE represents the change in T_C over time due to heat gained in the body from metabolic activity (input H_R) and heat lost to the skin due to blood flow. The second ODE represents the change in T_S over time due to heat gained in the skin from the body and heat lost to the environment via the difference between T_S and T_A and sweat evaporation (which depends on T_A, R_H, and individual factors, such as clothing, etc.). The mathematical model consists of three ODEs with seven parameters.

The first step is to determine a set of initial parameters and their corresponding SDs. For this purpose, we estimated the initial model parameters using data from all subjects (except for the test subject for whom we wished to estimate T_C) by fitting the model to these data so as to minimize the overall mean squared error between the model-estimated physiological variables H_R, T_S, and T_C and their corresponding measurements. Subsequently, we estimated the parameters' SDs. We repeated this procedure for each of the six subjects used in our study, thus obtaining six slightly different "group-average" models. We confirmed that all estimated parameters were within the expected range obtained from experimental studies and in agreement with previously published more detailed thermoregulatory models [14, 16, 17].

3.1.3 The Kalman Filter Algorithm

To implement the Kalman filter algorithm, we converted the three ODEs of the mathematical model to a discrete time-varying linear model with the model states consisting of H_R, T_S, T_C, and the model parameters. We initialized the Kalman filter with the group-average model parameters, their corresponding SDs, the noise variances of the H_R and T_S measurements obtained from the device specifications, and a measure of the

systemic uncertainty between the mathematical model estimates and a subject's data. We estimated the systemic uncertainty by using the first 5 min of the subject's data.

After initialization, the Kalman filter algorithm proceeded in the following manner. At each 15-s discrete time interval, the algorithm used the provided T_A and R_H, a 5-min moving average of the measured A_C at the current time point, and the model parameters estimated up to the previous time point to update the model states. Next, the algorithm used the error between the measured H_R and T_S and their corresponding model estimates to update the model states and parameters at the current time point. The algorithm repeated this procedure for each time-step until the end of the time-series data.

3.1.4 Evaluation of the Individualized Model

We evaluated two variants of the individualized model: *1*) one variant that used non-invasive measurements of A_C, H_R, and T_S along with hourly measurements of the environmental variables T_A and R_H (original model), and *2*) another variant that only used the measured A_C and H_R and month-average values of the environmental variables (T_A = 27.2°C and R_H = 77%; reduced model). The reduced model allowed us to evaluate model performance in cases where T_S measurements and hour-by-hour weather information are not available.

As discussed in above, we initialized the individualized model using a group-average parameter set obtained while excluding the test subject for whom we wished to estimate T_C. This allowed us to cross validate the model by comparing the measured and estimated T_C. We repeated the same cross-validation procedure six times to assess model performance for each of the six subjects. We used two metrics to assess the model estimations: the root mean squared error (RMSE) and the time delay between the measured and the estimated T_C. We computed the RMSE as the square root of the mean squared differences between the model-estimated T_C and the measured T_C across the time duration of the data. We computed the delay as the time difference between the maximum values of the auto-correlation of the measured T_C and the cross-correlation between the measured and the estimated T_C.

3.2 Results: T_C Estimation Using Non-Invasive Measurements

Figure 4 shows the performances of the two variants of the individualized model on one subject (subject #1). The top-left panel shows the measured A_C (gray dash-dot line) and its 5-min moving average (solid black line). The A_C drove the individualized model to track the measured H_R and T_S (middle and bottom panels, respectively) via the Kalman filter, and provided real-time T_C estimates (right panel). The original and reduced models estimated T_C with RMSEs of 0.21°C and 0.24°C and delays of 0 min and 1 min, respectively.

Table 2 shows the average RMSEs and estimation delays for the original and reduced models across the six subjects. The original and reduced models yielded average RMSEs of 0.31°C (SD 0.09) and 0.35°C (SD 0.10) and average estimation delays of 3 min (SD 4) and 5 min (SD 4), respectively. Thus, the reduced model yielded a 13% higher RMSE and a 2-min additional delay compared with the original model.

3.3 Discussion: T_C Estimation Using Non-Invasive Measurements

A novel feature of the individualized model is that it adapts the model parameters to a subject and, as such, explicitly accounts for subject-specific variations in thermoregulatory responses, acclimation, and responses to exogenous factors, such as clothing and environmental conditions. For example, if R_H increases or a subject's clothing impedes sweat evaporation, the model accounts for these changes by reducing the rate of heat loss due to sweat evaporation, leading to an increase in T_C. This is possible because the Kalman filter

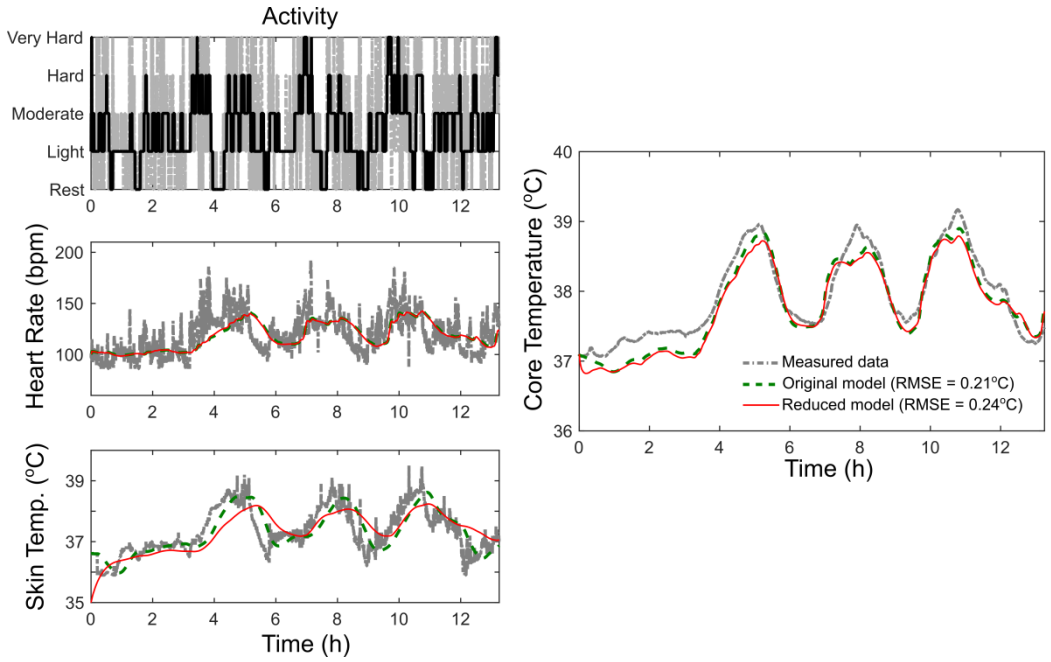

Figure 4: Performance of two variants of the individualized model on one subject (subject #1). The original model used the measured activity, heart rate [in beats/min (bpm)], and skin temperature along with hourly measurements of two environmental variables: ambient temperature and relative humidity. The reduced model used month-average values of the environmental variables and did not use the measured skin temperature. The top-left panel shows the measured activity (gray dash-dot line) and a 5-min moving average (solid line). The middle- and bottom-left panels show the measured heart rate and skin temperature, respectively, and the corresponding model estimates. The right panel shows the measured core temperature and the corresponding model estimates.

uses the non-invasive measurements of H_R and T_S to update the model parameters in real time and adapt them to subject-specific responses.

The two variants of the individualized model estimated T_C with errors of 0.31°C and 0.35°C and small delays of 3- to 5-min delay (Table 2). These errors are within the physiological variations of T_C in an individual (0.40°C) [18]. The estimation delays occurred mainly because of the inherent time lags associated with the low-pass filters used to smooth the H_R and T_S measurements. While an "optimal" algorithm should provide T_C estimates with no delay, we believe that such a requirement may not be practical for real-time applications

Table 2: Performances of the two variants of the individualized models across the six subjects. The original model estimated T_C using non-invasive measurements of A_C, H_R, and T_S and hourly measurements of T_A and R_H. The reduced model estimated T_C using non-invasive measurements of A_C and H_R and month-average values of T_A and R_H

Individualized models	RMSE (°C)	Delay (min)
Original model	0.31 (0.09)	3 (4)
Reduced model	0.35 (0.10)	5 (4)

Values are means (standard deviations). A_C, activity level; H_R, heart rate; R_H, relative humidity; T_A, ambient temperature; T_C, core body temperature; T_S, skin temperature.

when the time-series signal is noisy and needs to be further smoothed before use [5]. Moreover, a 3- to 5-min delay represents less than 15% of the time taken by T_C to rise by 1°C during physical activity [16]. Thus, the T_C estimates provided by the individualized model can be used as a surrogate for the ingestible pill and drive the alert algorithm detailed in Section 2.0. This could, for the first time, allow us to develop a hardware/software system for real-time warning of an impending heat injury.

Very few of the existing non-invasive performance- and fitness-tracking devices provide T_S measurements, e.g., Basis Peak™ (Intel Inc., San Francisco, CA). Hence, the observation that the reduced model that only requires H_R and A_C, which are readily available in many devices, was only 13% worse than the original model has an important ramification in the development of a reliable real-time warning system.

4.0 CONCLUSIONS

In conclusion, we developed an alert algorithm to provide reliable ahead-of-time warning of an impending rise in T_C. We showed that 20-min-ahead AR model predictions combined with the SPRT algorithm provides a sufficiently long effective prediction horizon (18 min), with a high sensitivity and specificity (> 87%) and a small number of decision switches (four) to enable preventive interventions to minimize the risk of heat injuries. We then developed an individualized model that uses non-invasive measurements of physiological signals and environmental variables to adapt the model parameters and provide subject-specific, individualized T_C estimates. We found that the individualized model provided accurate T_C estimates even when we used month-averaged values of the environmental variables and neglected skin temperature measurements. These findings suggest that the model-estimated T_C can replace the invasive core temperature measuring pill and thus enable the development of an early warning system that can be deployed in ambulatory settings. Currently, we are in the process of integrating this model with the alert algorithm in a smartphone application to provide reliable early warning of an impending rise in core temperature, which would help prevent heat injuries.

ACKNOWLEDGEMENTS

This study was supported by the Defense Medical Research and Development Program and by the Military Operational Medicine Research Area Directorate of the U.S. Army Medical Research and Materiel Command, Fort Detrick, MD.

DISCLAIMER

The opinions and assertions contained herein are the private views of the authors and are not to be construed as official or as reflecting the views of the U.S. Army or of the U.S. Department of Defense. This paper has been approved for public release with unlimited distribution.

REFERENCES

[1] Armed Forces Health Surveillance Center, "Update: heat injuries, active component, U.S. Armed Forces, 2010," *Med Surv Monthly Rep*, vol. 18, no. 3, pp. 6-8, Mar. 2011 [Online]. Available: http://www.afhsc.mil/documents/pubs/msmrs/2011/v18_n03.pdf#Page=6, accessed on 07/23/2015.

[2] Armed Forces Health Surveillance Center, "Update: heat injuries, active component, U.S. Armed Forces, 2013," *Med Surv Monthly Rep*, vol. 21, no. 3, pp. 10-13, Mar. 2014 [Online]. Available: https://www.afhsc.mil/documents/pubs/msmrs/2014/v21_n03.pdf#Page=10, accessed on 07/22/2015.

[3] Y. Epstein and W.O. Roberts, "The pathophysiology of heat stroke: an integrative view of the final

common pathway," *Scand J Med Sci Sports*, vol. 21, no. 6, pp. 742-748, Dec. 2011.

[4] C. Byrne and C. L. Lim, "The ingestible telemetric body core temperature sensor: a review of validity and exercise applications," *Br J Sports Med*, vol. 41, no. 3, pp. 126-133, Mar. 2007.

[5] A. Gribok, M. Buller, R. Hoyt, and J. Reifman, "A real-time algorithm for predicting core-temperature in humans," *IEEE Trans Inf Tech in Biomed*, vol. 14, no. 4, pp. 1039-1045, May 2010.

[6] S. Laxminarayan, M. Buller, W. Tharion, and J. Reifman, "Human core temperature prediction for heat-injury prevention," *IEEE J Biomed and Health Inf*, vol. 19, no. 3, pp. 883-891, May 2015.

[7] Y. Liu, S. H. Zhu, G. H. Wang, F. Ye, and P. Z. Li, "Validity and reliability of multiparameter physiological measurements recorded by the Equivital lifemonitor during activities of various intensities," *J Occup Environ Hyg*, vol. 10, no. 2, pp. 78-85, Aug. 2012.

[8] L. Marple, *Digital Spectral Analysis with Applications*, Englewood Cliffs, NJ: Prentice Hall, 1987.

[9] B. Efron and R. J. Tibshirani, *An Introduction to the Bootstrap*, London, UK: Chapman & Hall, 1993.

[10] A. V. Gribok, M. J. Buller, R. W. Hoyt, and J. Reifman, "Providing statistical measures of reliability for body core temperature predictions," *Proc Conf IEEE Eng Med Biol Soc*, pp. 545–548, Aug. 2007.

[11] A. Wald, "Sequential tests of statistical hypotheses," Ann Math Stat, vol. 16, pp. 117-186, 1945.

[12] L. Chen, A. T. Reisner, X. Chen, A. Gribok, and J. Reifman, "Are standard diagnostic test characteristics sufficient for the assessment of continual patient monitoring?" *Med Decis Making*, vol. 33, no. 2, pp. 225-234, Feb. 2013.

[13] R. E. Kalman, "A new approach to linear filtering and prediction problems," *J Fluids Engg*, vol. 82, no. 1, pp. 35-45, Mar. 1960.

[14] D. Fiala, K. J. Lomas, and M. Stohrer, "A computer model of human thermoregulation for a wide range of environmental conditions: the passive system," *J Appl Physiol*, vol. 87, no. 5, pp. 1957-1972, Nov. 1999.

[15] J. E. Sasaki, D. John, and P. S. Freedson, "Validation and comparison of ActiGraph activity monitors," *J Sci Med Sport*, vol. 14 no. 5, pp. 411-416, May 2011.

[16] C. A. Horswill, J. R. Stofan, S. C. Lovett, and C. Hannasch, "Core temperature and metabolic responses after carbohydrate intake during exercise at 30 degrees C," *J Athl Train*, vol. 43, no. 6, pp. 585-591, Oct-Dec 2008.

[17] E. D. Yildirim and B. Ozerdem, "A numerical simulation study for the human passive thermal system," *Energy and Buildings*, vol. 40, no. 7, pp. 1117-1123, Jul. 2008.

[18] G. Kelly, "Body temperature variability (part 1): a review of the history of body temperature and its variability due to site selection, biological rhythms, fitness, and aging," *Altern Med Rev*, vol. 11, no. 4, pp. 278-293, Dec. 2006.